



**SİVAS UNIVERSITY OF SCIENCE AND TECHNOLOGY
FACULTY OF ENGINEERING AND NATURAL SCIENCES**

ELECTRICAL AND ELECTRONICS ENGINEERING

**CONTROL SYSTEMS
EXPERIMENTS MANUAL**

Supervisor : Assoc. Prof. Hacı Mehmet GÜZEY
Prepared by : Assoc. Prof. Hacı Mehmet GÜZEY
Research Asst. İlhan ERDOĞAN

2025

SİVAS

Contents

| | | |
|----------|---|-----------|
| 1 | Experiment 1: Inverted Pendulum | 2 |
| 1.1 | Purpose and Learning Outcomes | 2 |
| 1.2 | Background Theory | 2 |
| 1.3 | LQR Design | 3 |
| 1.4 | Hybrid Control Architecture | 4 |
| 1.5 | Experimental Procedure | 4 |
| 2 | Experiment 2: Ball-and-Beam | 5 |
| 2.1 | Objectives | 5 |
| 2.2 | System Modelling | 5 |
| 2.3 | Controller Synthesis | 5 |
| 2.4 | Simulation and Validation | 6 |
| 3 | Experiment 3: Two-Degree-of-Freedom Helicopter | 7 |
| 3.1 | System Description and Coordinates | 7 |
| 3.2 | Linearised State-Space Model | 7 |
| 3.3 | Integral LQR Controller | 8 |
| 4 | Experiment 4: Ball-and-Plate | 9 |
| 4.1 | Kinematic Relations | 9 |
| 4.2 | Linearised Dynamics | 9 |
| 4.3 | P-Controller Analysis | 9 |
| A | Quick-Reference Checklists | 10 |
| B | 2-DoF Helicopter Pre-lab Questions | 10 |

1 Experiment 1: Inverted Pendulum

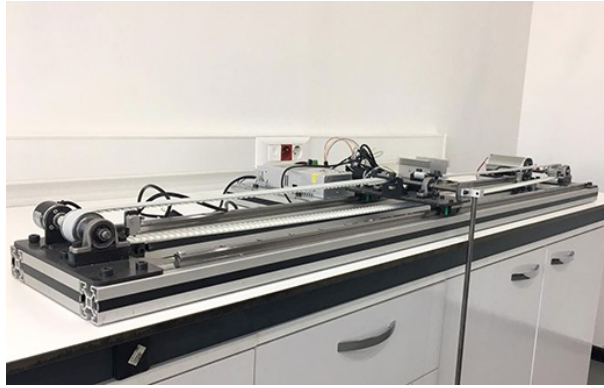


Figure 1: Quanser linear inverted pendulum setup.

1.1 Purpose and Learning Outcomes

The aim of this experiment is twofold:

- **Stabilisation and Tracking:** Design a state-feedback controller that balances the pendulum in its upright equilibrium *while simultaneously* tracking a commanded cart position.
- **Swing-up Control:** Devise an energy-based nonlinear controller that transfers the pendulum from its natural hanging configuration to the unstable upright equilibrium so that the stabilising controller can take over.

After completing this experiment you should be able to:

- Derive linear state-space models from Newton-Euler equations.
- Tune *Linear Quadratic Regulator* (LQR) gains and interpret the effect of the weighting matrices \mathbf{Q} and R .
- Implement hybrid control architectures (non-linear swing-up + linear stabilisation) in real hardware using QUARC/SIMULINK.

1.2 Background Theory

The inverted pendulum mounted on a cart is sketched in Fig. 1. The pivot is located on the cart, whose horizontal displacement is x_c ; the pendulum angle α is measured with respect to the *upright* position (i.e. $\alpha = 0$ corresponds to the vertical upward configuration).

Parameters

| | |
|----------|---|
| M_c | Mass of the cart (kg) |
| M_p | Mass of the pendulum (kg) |
| l_p | Distance from pivot to CoM (m) |
| J_p | Pendulum moment of inertia about its CoM (kg m ²) |
| B_{eq} | Equivalent viscous damping of cart (N s/m) |
| B_p | Viscous damping in the pendulum joint (N m s/rad) |

Equations of motion Using Lagrange's equations and linearising about $\alpha = 0$, the coupled dynamics read

$$\ddot{x}_c = \frac{1}{J_T} \left[-(J_p + M_p l_p^2) B_{eq} \dot{x}_c - M_p l_p B_p \dot{\alpha} + M_p^2 l_p^2 g \alpha + (J_p + M_p l_p^2) F_c \right], \quad (1)$$

$$\ddot{\alpha} = \frac{1}{J_T} \left[-M_p l_p B_{eq} \dot{x}_c - (J_{eq} + M_p) B_p \dot{\alpha} + (J_{eq} + M_p) M_p l_p g \alpha + M_p l_p F_c \right], \quad (2)$$

with

$$J_T = J_{eq} J_p + M_p J_p + J_{eq} M_p l_p^2, \quad J_{eq} = M_c + \frac{\eta_g K_g^2 J_m}{r_{mp}^2}. \quad (3)$$

The control force F_c is produced by the DC motor via the rack-and-pinion transmission and is ultimately driven by the motor voltage V_m .

State-space representation Define the state vector $\mathbf{x} = [x_c \ \alpha \ \dot{x}_c \ \dot{\alpha}]^T$ and choose the cart voltage $u \triangleq V_m$ as input. Then Eqs. (1)–(2) can be cast in the compact form

$$\dot{\mathbf{x}} = \mathbf{A} \mathbf{x} + \mathbf{B} u, \quad \mathbf{y} = \mathbf{C} \mathbf{x}, \quad (4)$$

where

$$\mathbf{A} = \frac{1}{J_T} \begin{bmatrix} 0 & 0 & J_T & 0 \\ 0 & 0 & 0 & J_T \\ 0 & M_p^2 l_p^2 g & -(J_p + M_p l_p^2) B_{eq} & -M_p l_p B_p \\ 0 & (J_{eq} + M_p) M_p l_p g & -M_p l_p B_{eq} & -(J_{eq} + M_p) B_p \end{bmatrix}, \quad \mathbf{B} = \frac{1}{J_T} \begin{bmatrix} 0 \\ 0 \\ J_p + M_p l_p^2 \\ M_p l_p \end{bmatrix}, \quad (5)$$

$$\mathbf{C} = \begin{bmatrix} 1 & 0 & 0 & 0 \\ 0 & 1 & 0 & 0 \end{bmatrix}, \quad \mathbf{D} = \mathbf{0}_{2 \times 1}. \quad (6)$$

1.3 LQR Design

Provided that (\mathbf{A}, \mathbf{B}) is controllable, the LQR problem consists in selecting symmetric weights $\mathbf{Q} = \text{diag}(q_1, q_2, q_3, q_4) > 0$ and $R > 0$ so as to minimise

$$J = \int_0^\infty (\mathbf{x}^T \mathbf{Q} \mathbf{x} + R u^2) dt. \quad (7)$$

The optimal feedback law is $u = -\mathbf{K} \mathbf{x}$ with

$$\mathbf{K} = R^{-1} \mathbf{B}^T \mathbf{P}, \quad \mathbf{A}^T \mathbf{P} + \mathbf{P} \mathbf{A} - \mathbf{P} \mathbf{B} R^{-1} \mathbf{B}^T \mathbf{P} + \mathbf{Q} = \mathbf{0}, \quad (8)$$

where \mathbf{P} is the unique positive-definite solution of the Algebraic Riccati Equation.

Tuning guidelines Increasing q_i accentuates the penalty on the corresponding state x_i and therefore amplifies the i -th column of \mathbf{K} . Conversely, enlarging R attenuates *all* gains uniformly, leading to slower but less aggressive control effort.

1.4 Hybrid Control Architecture

In practice, the LQR gains are activated only when $|\alpha| < \epsilon$ (typically $\epsilon = 10^\circ$). Otherwise a swing-up controller based on energy shaping drives the pendulum toward the upright equilibrium. A finite-state supervisor switches between the two controllers with hysteresis to avoid chattering.

1.5 Experimental Procedure

1. Open `setup_ip02_sip.m` and locate the LQR section. Initialise

$$\mathbf{Q} = \text{diag}(1, 1, 1, 1), \quad R = 0.1.$$

2. Run the script to compute the default \mathbf{K} . Simulate the closed-loop response using `s_ip02_sip.m`. Observe the cart displacement and pendulum angle.
3. Systematically vary R across an order of magnitude (0.01–1) and record the rise time, overshoot and control effort.
4. With R fixed to 0.1, tune each q_i individually (e.g. $1 \rightarrow 10$) and document the influence on \mathbf{K} and on the time response.
5. Iterate until the performance criteria below are satisfied while keeping $|V_m| \leq 10$ V:

| | |
|------------------------|---|
| Settling time (2 %) | $t_s < 2$ s |
| Maximum pendulum angle | $ \alpha _{\text{peak}} < 4^\circ$ |
| Cart position error | $ x_c - x_{c,d} < 2$ mm (steady state) |

6. Export the logged variables `data_xc`, `data_alpha`, `data_vm` and generate a publication-quality figure overlaying reference trajectories and measured signals.

A concise checklist for the lab session is provided in [Appendix A](#).

2 Experiment 2: Ball-and-Beam

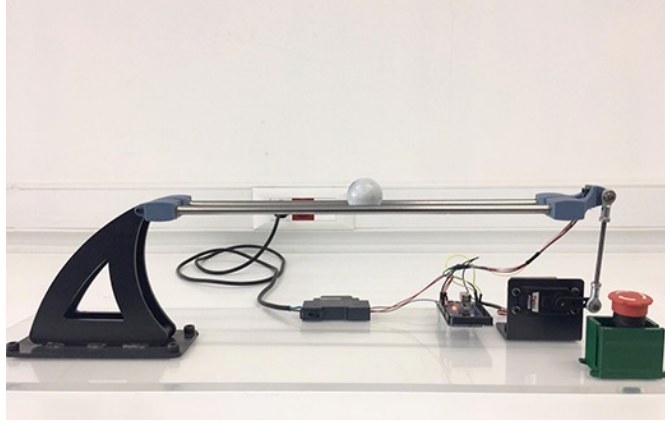


Figure 2: Electro-mechanical Ball-and-Beam apparatus.

2.1 Objectives

Stabilise a metallic ball at an arbitrary longitudinal position on a tilting beam by means of a rotary servo. Compare proportional (P) and proportional-derivative (PD) strategies against the following *time-domain* specifications:

$$\begin{array}{ll} \text{Steady-state error} & |e_{ss}| \leq 0.5 \text{ cm} \\ 4\% \text{ settling time} & t_s \leq 3 \text{ s} \\ \text{Percent overshoot} & \text{PO} \leq 5\%. \end{array}$$

2.2 System Modelling

The inner servo loop is accurately represented by the first-order transfer function

$$P_s(s) = \frac{\theta_l(s)}{V_m(s)} = \frac{K}{s(\tau s + 1)}, \quad K = 1.5 \text{ rad s}^{-1} \text{V}^{-1}, \quad \tau = 25 \text{ ms}. \quad (9)$$

Neglecting friction, the ball dynamics reduce to the double integrator

$$P_{bb}(s) = \frac{X(s)}{\theta_l(s)} = \frac{K_{bb}}{s^2}, \quad (10)$$

where K_{bb} is a geometric constant determined in the Pre-lab tasks.

Combining both subsystems yields the open-loop plant $G(s) = P_s(s)P_{bb}(s)$ of relative degree 3.

2.3 Controller Synthesis

A cascade architecture (Fig. 3) is adopted: the inner servo loop employs a fixed proportional gain $k_{p,s}$ chosen to ensure a bandwidth *one decade* higher than the outer loop. The

outer loop is a PD compensator with transfer function

$$C_{bb}(s) = K_c(s + z)H(s), \quad H(s) = \frac{\omega_f s}{s + \omega_f}, \quad \omega_f = 2\pi \cdot 5 \text{ rad/s}, \quad (11)$$

where $H(s)$ is a first-order high-pass filter preventing noise amplification.

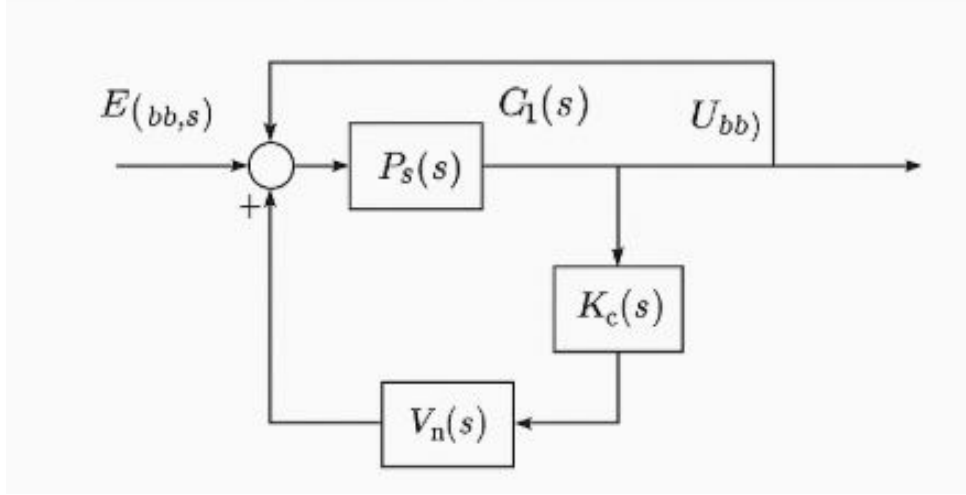


Figure 3: Cascade control structure for the Ball-and-Beam experiment.

Using the root-locus design rules for a second-order prototype with natural frequency ω_n and damping ratio ζ , the zero and proportional gain are initially selected via

$$z = \frac{\omega_n^2}{K_{bb}K_c}, \quad K_c = \frac{2\zeta\omega_n}{K_{bb}}. \quad (12)$$

Fine tuning is subsequently performed with the MATLAB `sisotool`.

2.4 Simulation and Validation

1. Define K_{bb} in the MATLAB workspace and launch `sisotool` with the open-loop plant $G(s)$.
2. Insert the target design requirements (PO and t_s) and manipulate (z, K_c) until the dominant poles lie within the admissible region.
3. Update `setup_ball_beam.m` with the new parameters and simulate the full cascade model. Typical responses are shown in Fig. 4.
4. Verify that voltage saturation ($|V_m| \leq 10 \text{ V}$) and angle constraints ($|\theta_l| \leq 56^\circ$) are respected.

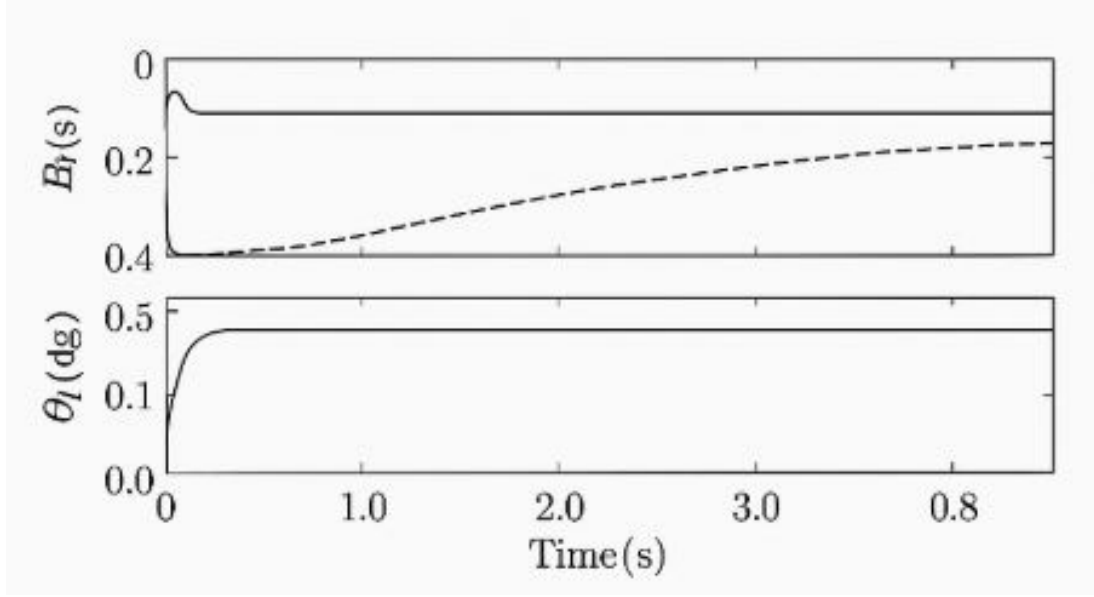


Figure 4: Simulated ball position (top), servo angle (middle) and motor voltage (bottom) for the tuned PD controller.

3 Experiment 3: Two-Degree-of-Freedom Helicopter

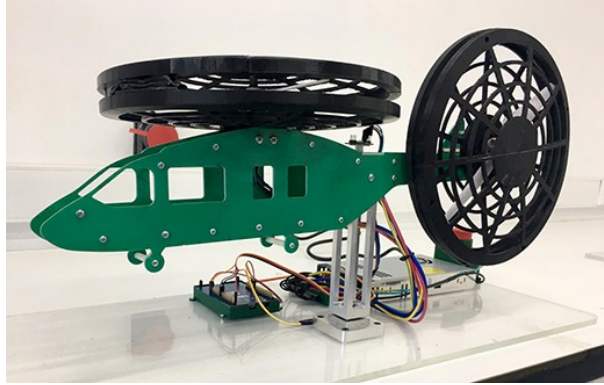


Figure 5: The Quanser 2-DoF laboratory helicopter.

3.1 System Description and Coordinates

The helicopter consists of a lightweight fuselage mounted on a pivot allowing independent *pitch* (θ) and *yaw* (ψ) rotations. Two brushless DC motors generate thrust forces F_p and F_y which, through lever arms, actuate the corresponding axes.

3.2 Linearised State-Space Model

With the state vector $\mathbf{x} = [\theta \ \psi \ \dot{\theta} \ \dot{\psi}]^T$ and the input $\mathbf{u} = [V_p \ V_y]^T$ (motor voltages), the linear model around the hover equilibrium reads

$$\dot{\mathbf{x}} = \mathbf{A}\mathbf{x} + \mathbf{B}\mathbf{u}, \quad \mathbf{y} = [\theta \ \psi]^T = \mathbf{C}\mathbf{x}. \quad (13)$$

The matrices \mathbf{A} and \mathbf{B} are given by

$$\mathbf{A} = \begin{bmatrix} 0 & 0 & 1 & 0 \\ 0 & 0 & 0 & 1 \\ 0 & 0 & -\frac{B_p}{J_{T,p}} & 0 \\ 0 & 0 & 0 & -\frac{B_y}{J_{T,y}} \end{bmatrix}, \quad \mathbf{B} = \begin{bmatrix} 0 & 0 \\ 0 & 0 \\ \frac{K_{pp}}{J_{T,p}} & \frac{K_{py}}{J_{T,p}} \\ \frac{K_{yp}}{J_{T,y}} & \frac{K_{yy}}{J_{T,y}} \end{bmatrix}, \quad (14)$$

where $J_{T,p} = J_{eq,p} + m_{heli}l_{cm}^2$ and $J_{T,y} = J_{eq,y} + m_{heli}l_{cm}^2$.

3.3 Integral LQR Controller

Augment the state with the integral of pitch and yaw errors:

$$\mathbf{x}_i = [\theta \quad \psi \quad \dot{\theta} \quad \dot{\psi} \quad \int \theta dt \quad \int \psi dt]^\top. \quad (15)$$

The feedback law $\mathbf{u} = -\mathbf{K}\mathbf{x}_i$ is obtained by solving the augmented LQR problem with

$$\mathbf{Q} = \text{diag}(200, 150, 100, 200, 50, 50), \quad \mathbf{R} = \mathbf{I}_2. \quad (16)$$

Resulting gains are

$$\mathbf{K} = \begin{bmatrix} 18.9 & 1.98 & 7.48 & 1.53 & 7.03 & 0.77 \\ -2.22 & 19.4 & -0.45 & 11.9 & -0.77 & 7.03 \end{bmatrix}. \quad (17)$$

Implementation hints, pre-lab questions and a structured testing protocol are provided in Appendix B.

4 Experiment 4: Ball-and-Plate

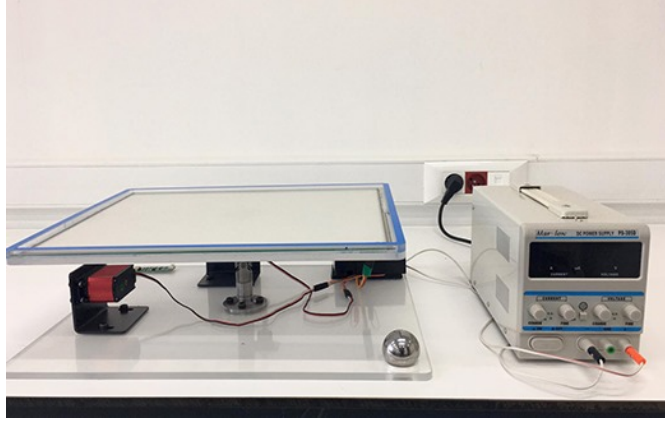


Figure 6: Ball-and-Plate platform.

4.1 Kinematic Relations

From the geometry in Fig. 6, the small-angle approximations yield

$$\sin \alpha = \frac{r_m}{L_x} \sin \theta_x \approx \frac{r_m}{L_x} \theta_x, \quad \sin \beta = \frac{r_m}{L_y} \theta_y. \quad (18)$$

4.2 Linearised Dynamics

Assuming rolling without slipping and linearising about the horizontal plane, the translational accelerations become

$$\ddot{x}b = K_{BBT,x} \theta_x, \quad K_{BBT,x} = \frac{m_b g r_b}{2r_m} \frac{1}{(m_b g r_b/2 + J_b)L_x}, \quad (19)$$

$$\ddot{y}b = K_{BBT,y} \theta_y, \quad K_{BBT,y} = \frac{m_b g r_b}{2r_m} \frac{1}{(m_b g r_b/2 + J_b)L_y}. \quad (20)$$

Thus each axis may be controlled independently via a cascade structure identical to the Ball-and-Beam, replacing $P_{bb}(s)$ by K_{BBT}/s^2 .

4.3 P-Controller Analysis

Using solely a proportional gain K_c in the outer loop, the closed-loop transfer function (y-axis) reads

$$T_y(s) = \frac{125K_c}{0.01s^3 + s^2 + 125K_c}. \quad (21)$$

Root-locus inspection (Fig. 7) reveals that for all $K_c > 0$ a pair of poles remains in the right half-plane, rendering the closed loop unstable. Consequently, at least a derivative term (PD) is required to stabilise the plate.

Detailed controller synthesis (e.g., state feedback with integral action) is left as an extension exercise.

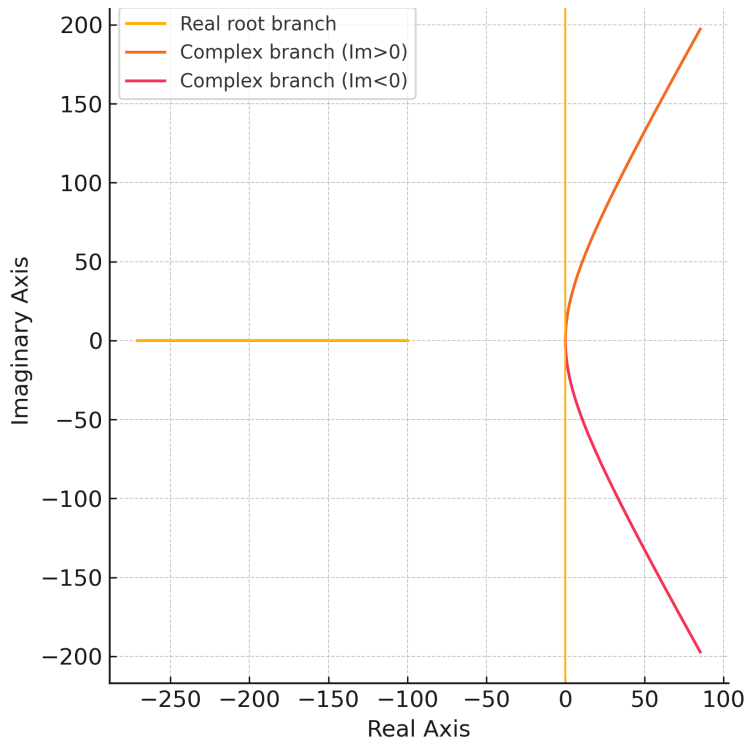


Figure 7: Root locus of the Ball-and-Plate outer loop with pure P control.

A Quick-Reference Checklists

B 2-DoF Helicopter Pre-lab Questions

1. Identify the two controlled degrees of freedom and interpret their physical meaning.
2. Provide concise definitions of *feedback* and *feedforward*. Discuss why both may be beneficial in aerial systems.
3. List the measurable signals available on the Quanser helicopter and explain how they feed into the state-feedback law.
4. Outline the effect of B_p and B_y on the closed-loop damping. Suggest experimental methods for estimating these parameters.